PCP
PLANT & CELL PHYSIOLOGY

Regulated *AtHKT1* Gene Expression by a Distal Enhancer Element and DNA Methylation in the Promoter Plays an Important Role in Salt Tolerance

Dongwon Baek[1,3], Jiafu Jiang[1,3], Jung-Sung Chung[1,3], Bangshing Wang[1], Junping Chen[2], Zhanguo Xin[2] and Huazhong Shi[1,*]

[1]Department of Chemistry and Biochemistry, Texas Tech University, Lubbock, TX 79409, USA
[2]Plant Stress and Germplasm Development Unit, USDA-ARS, Lubbock, TX 79415, USA
[3]These authors contributed equally to this work
*Corresponding author: E-mail, huazhong.shi@ttu.edu; Fax, +1-806-742-1289
(Received October 18, 2010; Accepted November 16, 2010)

Through *sos3* (salt *o*verly *s*ensitive 3) suppressor screening, two allelic suppressor mutants that are weak alleles of the strong *sos3* suppressor *sos3hkt1-1* were recovered. Molecular characterization identified T-DNA insertions in the distal promoter region of the *Arabidopsis thaliana HKT1* (*AtHKT1*, *At4g10310*) in these two weak *sos3* suppressors, which results in physical separation of a tandem repeat from the proximal region of the *AtHKT1* promoter. The tandem repeat is approximately 3.9 kb upstream of the ATG start codon and functions as an enhancer element to promote reporter gene expression. A putative small RNA target region about 2.6 kb upstream of the ATG start codon is heavily methylated. CHG and CHH methylation but not CG methylation is significantly reduced in the small RNA biogenesis mutant *rdr2*, indicating that non-CG methylation in this region is mediated by small RNAs. Analysis of *AtHKT1* expression in *rdr2* suggests that non-CG methylation in the putative small RNA target region represses *AtHKT1* expression in shoots. The DNA methylation-deficient mutant *met1-3* has nearly complete loss of total cytosine methylation in the putative small RNA target region and is hypersensitive to salt stress. The putative small RNA target region and the tandem repeat are essential for maintaining *AtHKT1* expression patterns crucial for salt tolerance.

Keywords: AtHKT1 • DNA methylation • Enhancer element • Gene regulation • Salt stress.

Abbreviatons: GUS, β-glucuronidase; MS, Murashige and Skoog; RdDM, RNA-directed DNA methylation; siRNA, small interfering RNA; TAIL-PCR, thermal asymmetric interlaced PCR.

Introduction

Plants cope with sodium toxicity by minimizing sodium accumulation in the shoots at the whole plant level (Munns and Tester 2008). At the cellular level, salt tolerance mechanisms function to reduce sodium accumulation in the cytoplasm through limiting sodium entry into the cell, actively transporting sodium out of the cell, and compartmentalizing sodium into the vacuole (Shi et al. 2005). In Arabidopsis, the plasma membrane Na^+/H^+ antiporter SOS1 (Salt Overly Sensitive 1, At2g01980) functions in Na^+ efflux by reducing Na^+ accumulation in the cytosol (Shi et al. 2000, Shi et al. 2002, Shi et al. 2003). SOS1 may also serve as an early signaling component to modulate apoplastic pH and the production of reactive oxygen species that trigger the downstream signaling events and responses (Chung et al. 2008). Transporters responsible for compartmentalization of Na^+ into the vacuole are thought to include the toloplast Na^+/H^+ antiporters (Blumwald et al. 2000). The Arabidopsis vacuolar Na^+/H^+ exchanger AtNHX1 (At5g27150) confers salt tolerance to yeast and plant cells by sequestering Na^+ into the vacuole, which supports vacuolar Na^+ compartmentation as one of the important salt tolerance mechanisms in plants (Apse et al. 1999, Gaxiola et al. 1999, Zhang and Blumwald 2001, Zhang et al. 2001).

Loss-of-function analysis of Arabidopsis and wheat *HKT1* genes established that HTK1 transports Na^+ into the cell and may control Na^+ uptake in roots (Rus et al. 2001, Laurie et al. 2002, Mäser et al. 2002, Rus et al. 2004). Two genetic screenings for mutations altering salt accumulation and tolerance in Arabidopsis have revealed the important role of AtHKT1 in salt tolerance. A screen of *sos3* suppressors identified eight *hkt1* mutant alleles that suppress the *sos3* NaCl-sensitive phenotype (Rus et al. 2001). The *hkt1* mutation also suppresses the Na^+ sensitivity of *sos1* and *sos2* mutants, suggesting that AtHKT1 works in coordination with SOS proteins to control Na^+ and K^+ homeostasis (Rus et al. 2004). Another genetic screening for mutants with sodium overaccumulation in shoot (*sas*) identified two allelic recessive mutants of Arabidopsis, *sas2-1* and *sas2-2*, and subsequent map-based gene cloning revealed

Plant Cell Physiol. 52(1): 149–161 (2011) doi:10.1093/pcp/pcq182, available FREE online at www.pcp.oxfordjournals.org

that the *sas2* locus corresponds to the *AtHKT1* gene (Nublat et al. 2001, Berthomieu et al. 2003). Based on genetic and molecular analyses of the *sas2* mutant, Berthomieu et al. (2003) concluded that AtHKT1 is involved in shoot to root Na^+ recirculation, probably by mediating Na^+ loading into the phloem sap in shoots and unloading in roots. However, studies with null *hkt1* mutants by Sunarpi et al. (2005) led to the conclusion that AtHKT1 mediates unloading of Na^+ in the xylem sap of Arabidopsis in the presence of high salinity. In a recent study, Davenport et al. (2007) have established that AtHKT1 mediates neither shoot to root Na^+ recirculation nor Na^+ influx into roots; rather, AtHKT1 seems to direct retrieving Na^+ from the xylem and loading of Na^+ into root vacuoles. It now appears that the primary role of AtHKT1 is to retrieve Na^+ from the xylem in roots to reduce transport of Na^+ from roots to shoots (Munns and Tester 2008, Horie et al. 2009, Plett and Møller 2010). However, the major role of AtHKT1 in leaves still remains elusive. The complication in interpretation of AtHKT1 function in salt tolerance could be due to as yet unknown features of *AtHKT1* gene expression and regulation. In fact, Møller et al. (2009) recently showed that overexpression of AtHKT1 specifically in the mature root stele increases salt tolerance in transgenic plants, while overexpression of AtHKT1 driven by the 35S promoter in whole plants results in salt hypersensitivity. Therefore, understanding tissue-specific expression of AtHKT1 and its control mechanisms appears to be important for uncovering AtHKT1 function on a whole plant level.

DNA methylation has long been known to regulate gene expression. Cytosine residues in a DNA molecule can be methylated in three different sequence contexts, i.e. CG, CHG and CHH (H = A, T or C). In Arabidopsis, de novo cytosine methylation is carried out by the methyltransferases DRM1 and DRM2, while the methyltransferase MET1 and chromomethylase CMT3 maintain CG and CHG methylation (Henderson and Jacobsen 2007). New studies, however, suggested that MET1 and CMT3 may also be important for de novo methylation in some genomic regions (Gehring and Henikoff 2008). De novo methylation in many genomic regions is guided by small RNAs in a process called RNA-directed DNA methylation (RdDM). Small RNAs target the DNA sequences to trigger DNA methylation using an as yet unknown mechanism. Biogenesis of small interfering RNAs (siRNAs) requires the activity of PolIV, RDR2 and DCL3; and RdDM requires AGO4, PolV, DRD1 and DRM2 (Xie and Qi 2008, Wierzbicki et al. 2008).

Here we present a study on *AtHKT1* gene expression and its regulation. We found that a distal enhancer element and small RNA-mediated DNA methylation are involved in tissue-specific and regulated expression of *AtHKT1*, which play an important role in Arabidopsis salt tolerance. Our findings are expected to allow for a better understanding of the role of AtHKT1 in control of Na^+ transport on a whole plant level.

Results

Identification of *sos3* suppressors

From 65,000 individual T-DNA insertion lines generated in the *sos3* genetic background, 15 putative mutants showing suppression of the *sos3* salt-hypersensitive phenotype were identified. Among these suppressor mutants, four mutants displayed strong suppression of *sos3* salt sensitivity and harbored mutations in the *AtHKT1* gene, and thus were designated as *sos3hkt1-1* to *sos3hkt1-4* (Rus et al. 2001, Rus et al. 2004). The other 11 suppressor mutants showed a relatively weak salt suppression phenotype compared with *sos3hkt1-1*. The two weak *sos3* suppressors *992* and *1425*, which were later designated as *sos3hktInsP-1* (*hkt1* Insertion in Promoter) and *sos3hktInsP-2* after molecular identification of the mutations in these two lines, were subjected to further study. As shown in **Fig. 1a and b**, the weak suppressor *sos3hktInsP-1* displayed clear suppression of *sos3* salt sensitivity at the concentration of 60 mM NaCl but showed very little suppression when NaCl was elevated to 75 mM, while the strong *sos3* suppressor *sos3hkt1-1* exhibited apparent suppression of *sos3* salt sensitivity up to 75 mM NaCl. The single mutant *hkt1-1* resembled the wild-type seedlings in root growth at different concentrations of NaCl, but leaf growth of *hkt1-1* was more inhibited than in wild-type seedlings at higher concentrations (100 and 125 mM) of NaCl (**Fig. 1a**). These results indicated that *sos3hktInsP-1* is a weaker suppressor compared with *sos3hkt1-1* and is phenotypically distinguishable from the *sos3* mutant in response to salt stress.

Na^+ accumulation in *sos3* suppressors

When compared with wild-type plants, *sos3* mutant plants accumulated higher Na^+ in both shoots and roots after NaCl treatment (**Fig. 1c**), which supports the observation that both *sos3* roots and leaves are more NaCl sensitive than wild-type plants (**Fig. 1a**). In shoots, Na^+ content in the *hkt1-1* single mutant was significantly higher than in the wild type, but in roots, the difference between *hkt1-1* and wild-type plants was only marginal (**Fig. 1c**). This result is consistent with *hkt1-1* leaves but not roots being more sensitive to salt stress (**Fig. 1a**). Interestingly, the *hkt1-1* mutation in the background of *sos3* (*sos3hkt1-1*) results in reduced Na^+ accumulation in both shoots and roots compared with the *sos3* single mutant (**Fig. 1c**). Na^+ accumulation in shoots and roots of the weak *sos3* suppressor line *sos3hktInsP-1* was also reduced compared with that in the *sos3* mutant (**Fig. 1c**). Thus, suppression of *sos3* salt sensitivity by the *hkt1-1* mutation could be caused at least in part by limiting Na^+ entry into the plant. Consistent with this notion, the *sos3* mutant had higher Na^+ content in the xylem sap than the wild type, but this increase was significantly reduced in the strong suppressor line *sos3hkt1-1* and marginally reduced in the weak suppressor line *sos3hktInsP-1* (**Fig. 1c**). The *hkt1-1* single mutant also accumulated more Na^+ in xylem sap than the wild type (**Fig. 1c**). Na^+ content in

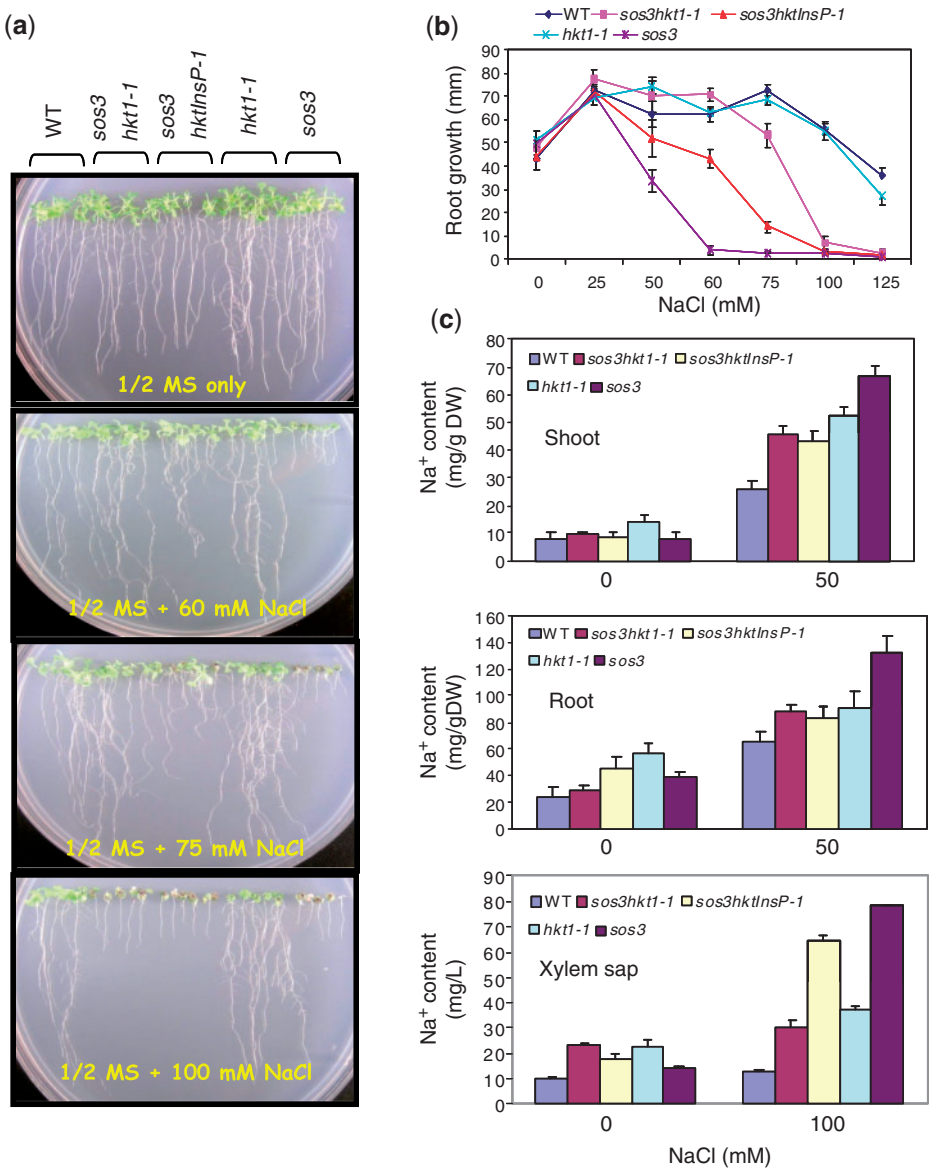

Fig. 1 Characterization of a weak *sos3* suppressor. (a) Root growth of the wild type (WT), *sos3hkt1-1*, *sos3hktInsP-1*, *hkt1-1* and *sos3* in agar medium supplemented with different concentrations of NaCl. Four-day-old seedlings grown in 1/2 MS agar medium were transferred to a medium with the indicated NaCl concentration. Pictures were taken on the 10th day after transfer. (b) Quantitative measurements of root growth at different concentrations of NaCl. Data represent the average root length of five seedlings. (c) Na^+ content in shoot, root and xylem sap. Plants were hydroponically cultured and root and shoot were separated for ion content measurement. Error bars represent the SD ($n = 3$).

shoots, roots and xylem sap of the weak suppressor line *sos3hktInsP-1* was relatively higher than that in the strong suppressor line *sos3hkt1-1*, which may account for the weak suppression phenotypes.

T-DNA insertions in the promoter of the *AtHKT1* gene in the weak suppressors are responsible for the suppression phenotype

Thermal asymmetric interlaced PCR (TAIL-PCR) revealed that the weak suppressor 992 (*sos3hktInsP-1*) possesses a T-DNA insertion in the promoter approximately 3.6 kb upstream of the ATG start codon of the *AtHKT1* gene (**Fig. 2a**). However, TAIL-PCR failed to generate sequence information regarding the T-DNA insertions in the *sos3hktInsP-2* suppressor. An allelism test indicated that these two suppressors are allelic (**Fig. 2b**), which suggests that a mutation is also located in the *AtHKT1* gene in *sos3hktInsP-2*. Using a specific primer for the border sequence of the T-DNA and primers targeting the entire *AtHKT1* gene including about 6.0 kb of the promoter region, PCR fragments were amplified from *sos3hktInsP-2* and sequenced. Sequence analysis indicated that a complex T-DNA insertion is located in the promoter of *AtHKT1* approximately

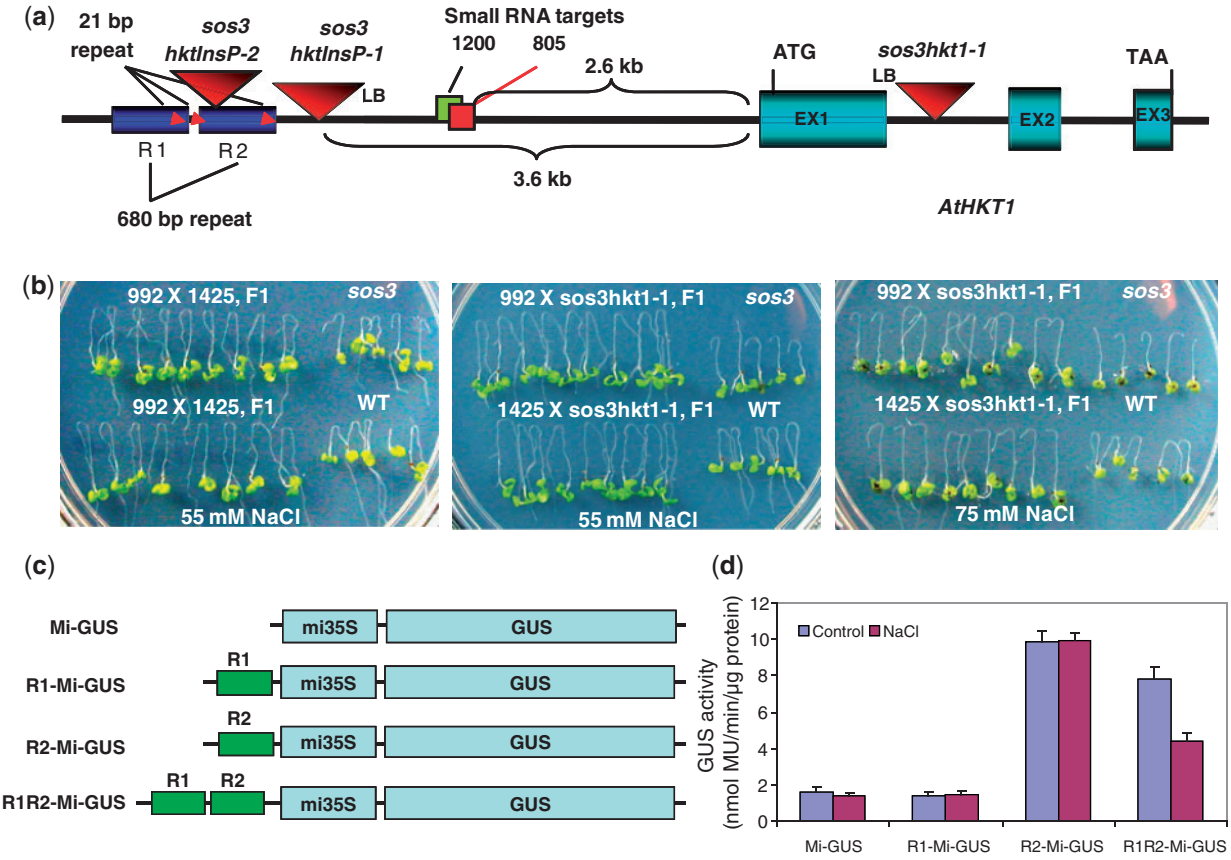

Fig. 2 Detection of T-DNA insertions in *sos3* suppressors and characterization of the tandem repeat of the *AtHKT1* promoter. (a) A diagram showing the T-DNA insertions in *992* (*sos3hktInsP-1*), *1425* (*sos3hktInsP-2*) and *sos3hkt1-1*. Also showing are complex structures of the *AtHKT1* promoter including a tandem repeat, 21 nt repeats within the tandem repeat and a putative small RNA target site. (b) Allelism test among *992*, *1425* and *sos3hkt1-1*. A root bending assay was used to test the sensitivity of the seedlings to NaCl. (c) A diagram showing the constructs used for Arabidopsis transformation and GUS assay to dissect the function of the tandem repeat. (d) Quantitative GUS activity measurement of the transgenic seedlings. NaCl, 200 mM NaCl treatment for 5 h.

4.5 kb upstream of the ATG start codon (**Fig. 2a**). To further verify whether the T-DNA insertions are responsible for the suppressor phenotype, *sos3hktInsP-1* and *sos3hktInsP-2* were crossed with *sos3hkt1-1* and the resulting F_1 seeds were subjected to salt sensitivity tests. F_1 seedlings displayed a suppression phenotype at 55 mM NaCl but failed to suppress *sos3* salt sensitivity at 75 mM NaCl, at which point *sos3hkt1-1* still exhibited strong suppression of *sos3* salt sensitivity (**Fig. 2b**). This result indicated that both *sos3hktInsP-1* and *sos3hktInsP-2* are weak alleles of *sos3hkt1-1*, further supporting the idea that T-DNA insertions in *sos3hktInsP-1* and *sos3hktInsP-2* are indeed responsible for suppression of *sos3* salt sensitivity. To exclude the possibility that other mutations in *AtHKT1* may contribute to the suppression phenotype, the entire coding region plus approximately 6.0 kb of the promoter region in *sos3hktInsP-1* and *sos3hktInsP-2* was sequenced and no mutations were found in these two suppressor lines.

Complex features of the *AtHKT1* promoter

T-DNA insertions in the distal promoter region of *AtHKT1* that conferred a weak suppression phenotype suggested an essential role for the upstream sequences of the T-DNA insertions. Sequence analysis revealed a tandem repeat present in the distal promoter region located about 3.9 kb upstream of the ATG start codon (**Fig. 2a**). Each repeat contains approximately 680 nt and is separated by 34 nt. The upstream repeat (repeat 1, R1) and the downstream repeat (repeat 2, R2) are nearly identical, with nine nucleotide substitutions and a few small deletions between these two repeat sequences (Supplementary Fig. S1a). The T-DNA insertion in *sos3hktInsP-1* separates the tandem repeat from the proximal promoter region and results in a partial loss of function of AtHKT1, which suggests that this tandem repeat plays a role in the regulation of *AtHKT1* expression. Moreover, a search for small RNA targets (Arabidopsis thaliana Small RNA Project, ASRP database, http://asrp.cgrb.oregonstate.edu) in the promoter of *AtHKT1* identified several regions located 2.0 kb upstream of the ATG start codon as potential targets of small RNAs. The sequence GATCTGGTG GTTGTGATGGTGGAGAT located about 2.6 kb upstream of the ATG start codon is complementary to two small RNA species, ASRP-805 and ASRP-1200, present in the ASRP database (**Fig. 2a**). Interestingly, a search for DNA methylation against

the methylome database (http://signal.salk.edu/cgi-bin/methylome) indicated that the promoter region potentially targeted by ASRP-805 and ASRP-1200 is heavily methylated.

The tandem repeat acts as an enhancer element

To determine the role of the tandem repeat in gene regulation, each repeat element and the tandem repeat were fused with a minimal 35S promoter driving β-glucuronidase (GUS) gene expression and the resulting constructs were introduced into Arabidopsis (**Fig. 2c**). Stable T_2 transformants were analyzed by histochemical staining (data not shown) and GUS activity assays. Transgenic plants harboring the 35S minimal promoter–GUS (Mi–GUS) or repeat 1-minimal 35S promoter–GUS (R1-Mi–GUS) displayed undetectable GUS activity by histochemical staining, while transgenic plants harboring repeat 2-minimal 35S promoter–GUS (R2-Mi–GUS) or tandem repeat-minimal 35S promoter–GUS (R1R2-Mi–GUS) exhibited strong GUS staining (data not shown). Enhanced expression of GUS gene by R2 and R1R2 was further confirmed by enzyme activity assays (**Fig. 2d**). Interestingly, the enhancement of GUS gene expression by R2 was stronger than that by the tandem repeat R1R2, which suggests that R1 may have inhibitory effect on R2 for the enhancement of gene expression. Furthermore, NaCl treatment did not affect R2-enhanced expression of GUS but reduced GUS expression driven by R1R2 (**Fig. 2d**), which suggests that R1 may be a NaCl-responsive element.

Non-CG methylation of the putative small RNA target region in the *AtHKT1* promoter is small RNA dependent

Heavy cytosine methylation was detected in the region of approximately 250 nt housing the putative small RNA target sequences (**Fig. 3a**). In this 250 bp region, cytosine methylation at CG sites was 95.6% in leaves and 84.9% in roots of wild-type seedlings (**Fig. 3a**). CG methylation in the leaves and roots of the *rdr2* mutant defective in small RNA biogenesis was not significantly different from that in the wild-type line (**Fig. 3a**). However, CG methylation in the *met1-3* null mutant was significantly reduced to very low levels, which is consistent with the role of Met1 being required for CG methylation in the genome. CHG and CHH methylation significantly decreased in both leaves and roots of the *rdr2* mutant (**Fig. 3a**). CHG methylation in the leaves and roots of *rdr2* was reduced to 21.7 and 23.4% compared with 48.5% in the leaves and 59.7% in roots of wild-type plants; CHH methylation was 3.8% in the leaves and 5.8% in roots of the *rdr2* mutant compared with 26.9% in leaves and 15.1% in roots of wild-type seedlings (**Fig. 3a**). These results indicate that non-CG methylation, in particular asymmetric CHH methylation in the *AtHKT1* promoter, is mediated by small RNAs generated through the RDR2 pathway. In the *met1-3* mutant, CHG methylation was completely abolished and CHH methylation was also substantially reduced in both leaves and roots (**Fig. 3a**). Thus, the

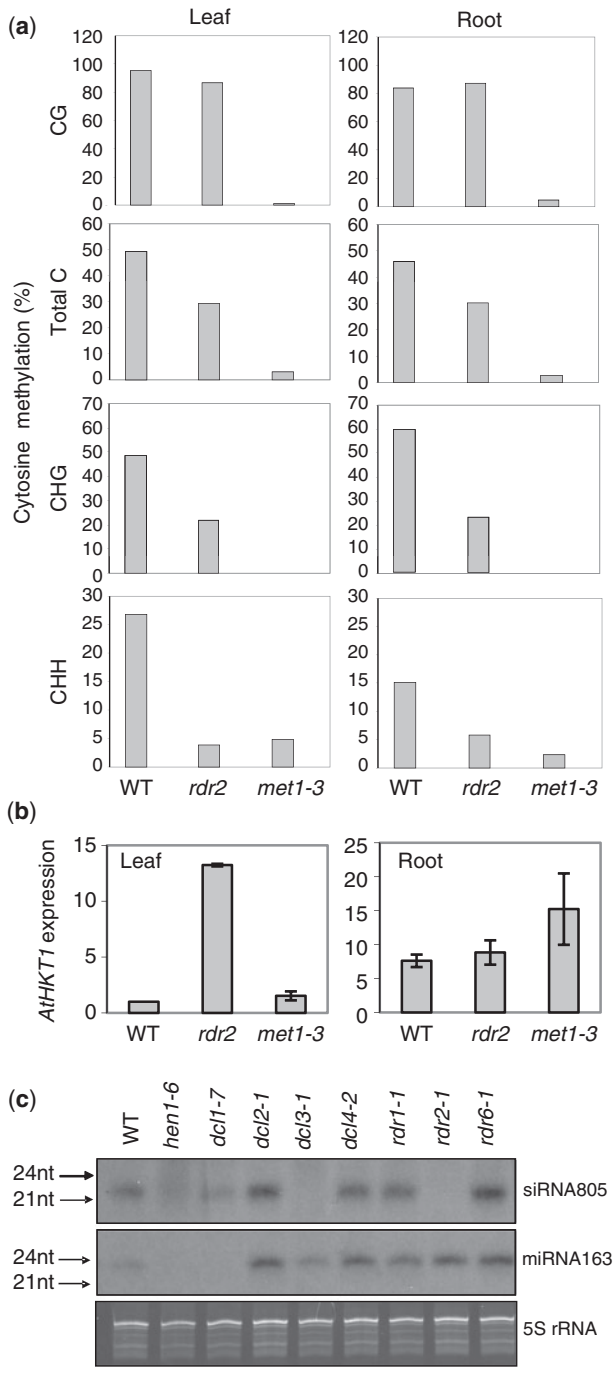

Fig. 3 Cytosine methylation, *AtHKT1* expression and small RNA detection. (a) CG, total cytosine, CHG and CHH methylation in the leaf and root of the wild type (WT), and *rdr2* and *met1-3* mutants. H = A, T or C. (b) Detection of *AtHKT1* transcript levels in leaf and root of the WT, *rdr2* and *met1-3* by real-time PCR. The expression level was calculated as the level relative to the value of the wild-type leaf. (c) The abundance of ASRP-805 in WT and different small RNA- and microRNA-related mutants. A 10 μg aliquot of RNA isolated from the leaves of 6-week-old plants grown in soil was used for Northern blotting. A size marker of 21 and 24 nt RNA oligos is shown on the left side. 5S rRNA stained by ethidium bromide is shown as a loading control.

met1-3 mutant possesses a nearly non-methylated form and *rdr2* possesses a reduced non-CG-methylated form at the putative small RNA target region of the *AtHKT1* promoter.

To assess the effects of reduced DNA methylation on *AtHKT1* expression, *AtHKT1* transcript levels were determined in the roots and leaves of wild-type, *rdr2* and *met1-3* lines (**Fig. 3b**). In wild-type seedlings, *AtHKT1* expression in roots is much higher than that in leaves, indicating a differential expression of *AtHKT1* in roots and leaves. *AtHKT1* transcript levels in the leaves of the *rdr2* mutant are substantially higher than that in the leaves of wild-type plants, while the roots of *rdr2* have similar *AtHKT1* transcript levels when compared with the wild-type. These results suggest that small RNA-mediated non-CG methylation in the *AtHKT1* promoter represses *AtHKT1* transcription in leaves but does not affect *AtHKT1* expression in roots. In the *met1-3* mutant in which total cytosine methylation is nearly abolished, *AtHKT1* transcript levels in roots increase >2-fold and are approximately 1.5-fold higher in leaves when compared with that in wild-type plants (**Fig. 3b**). Thus, heavy methylation of the *AtHKT1* promoter appears to inhibit its transcription in both leaves and roots.

Reduced non-CG methylation in the *rdr2* mutant suggested that RDR2-dependent small RNAs play an essential role in the methylation of the putative small RNA target sequence in the *AtHKT1* promoter. Consistent with being annotated as a small RNA in the ASRP database, the small RNA ASRP-805 (23 nt) complementary to the *AtHKT1* promoter sequence was detected in the wild type and in *dcl1*, *dcl2* and *dcl4* mutants, but not in small RNA biogenesis mutants *hen1*, *dcl3* and *rdr2* (**Fig. 3c**). In contrast, the known microRNA mi163 (24 nt) was detectable in *dcl3* and *rdr2* mutants but its biogenesis was apparently abolished in *hen1* and *dcl1* mutants in which microRNA biogenesis is blocked (**Fig. 3c**). This result reveals that ASRP-805 does exist in Arabidopsis as a small RNA species and its biogenesis is indeed RDR2 dependent.

Promoter without the tandem repeat and putative small RNA target region directed an altered expression pattern of *AtHKT1* and resulted in NaCl hypersensitivity

Previous reports have used an approximately 2.0 kb promoter region upstream of the ATG start codon of *AtHKT1* to study *AtHKT1* expression and function (Mäser et al. 2002, Berthomieu et al. 2003, Rus et al. 2004). However, our results imply that the sequences upstream of the 2.0 kb region of the *AtHKT1* promoter are required for full expression or regulation of *AtHKT1* expression. To determine whether the 2.0 kb promoter region is sufficient for full functional expression of *AtHKT1*, a construct, designated as *AtHKT1P-2.0kb:AtHKT1* including about 2.0 kb of the promoter region, the entire *AtHKT1* coding region with both exons and introns, and approximately 500 bp sequence downstream of the *AtHKT1* gene, was cloned into a plant binary vector and introduced into the strong *sos3* suppressor *sos3hkt1-1*. Two independent homozygous transgenic lines with a single copy of the transgene, designated 5-2 and 12-2, were selected for a complementation test. As shown in **Fig. 4a and b**, both 5-2 and 12-2 exhibited even greater NaCl sensitivity when compared with the *sos3* mutant. The root growth of 5-2 and 12-2 was almost completely inhibited at 20 mM NaCl, while the *sos3* mutant only showed a slight reduction in root growth. At 40 mM NaCl, the leaves of 5-2 and 12-2 were bleached, while the leaves of the *sos3* mutant remained green at NaCl concentrations even higher than 60 mM (**Fig. 4a**). Since the functional *AtHKT1* expression in 5-2 and 12-2 comes solely from the transgene *AtHKT1P-2.0kb:AtHKT1*, the phenotypes observed in these two transgenic lines can be attributed to altered *AtHKT1* expression patterns and mis-regulated expression of *AtHKT1*. To test this hypothesis, *AtHKT1* expression in the wild type, *sos3*, *sos3hkt1-1*, 5-2 and 12-2 lines was determined by real-time PCR (**Fig. 4c**). In contrast to the expression pattern of *AtHKT1* in the wild-type line in which *AtHKT1* expression is higher in root than in leaf, both 5-2 and 12-2 lines displayed substantially higher expression in leaves than in roots. Moreover, the transcript level of *AtHKT1* in leaves of these two transgenic lines was >100-fold higher than that in the wild type, while transcript levels of *AtHKT1* in roots of these two lines were similar to those in the roots of wild-type plants. These results indicate that the approximately 2.0 kb promoter region is able to drive the expression of *AtHKT1*, but is not functional as a native promoter, which further supports that sequences upstream of the 2.0 kb promoter region are necessary for *AtHKT1* regulation. Ion content measurements revealed that, after challenge with 50 mM NaCl for 1 d, both the 5-2 and 12-2 lines accumulated significantly higher Na^+ in leaves when compared with the wild type and *sos3* mutant plants (**Fig. 4d**). Without salt treatment, the potassium content in roots of 5-2 and 12-2 lines was substantially lower than that in wild-type and *sos3* mutant roots (data not shown). With salt treatment, the potassium content in roots of the 5-2 and 12-2 lines was much lower than that in wild-type roots (data not shown). Thus, the hypersensitive to NaCl phenotype of 5-2 and 12-2 may be attributed to mis-regulated expression of *AtHKT1*, which disrupts Na^+ and K^+ homeostasis in both roots and leaves.

DNA methylation in the putative small RNA target region is important for *AtHKT1* expression and salt tolerance

As an attempt to correlate DNA methylation, *AtHKT1* expression and salt tolerance, salt sensitivity of *met1-3* and *rdr2* was analyzed by using a root bending assay. The *met1-3* mutant displayed an apparent salt-sensitive phenotype in root growth (**Fig. 5a** and Supplementary Fig. S2a), which suggests that methylation in the putative small RNA target region and its regulated *AtHKT1* expression are likely to contribute to salt tolerance in Arabidopsis. However, *rdr2* showed a similar response to different concentrations of NaCl when compared with wild-type plants (data not shown). To establish further

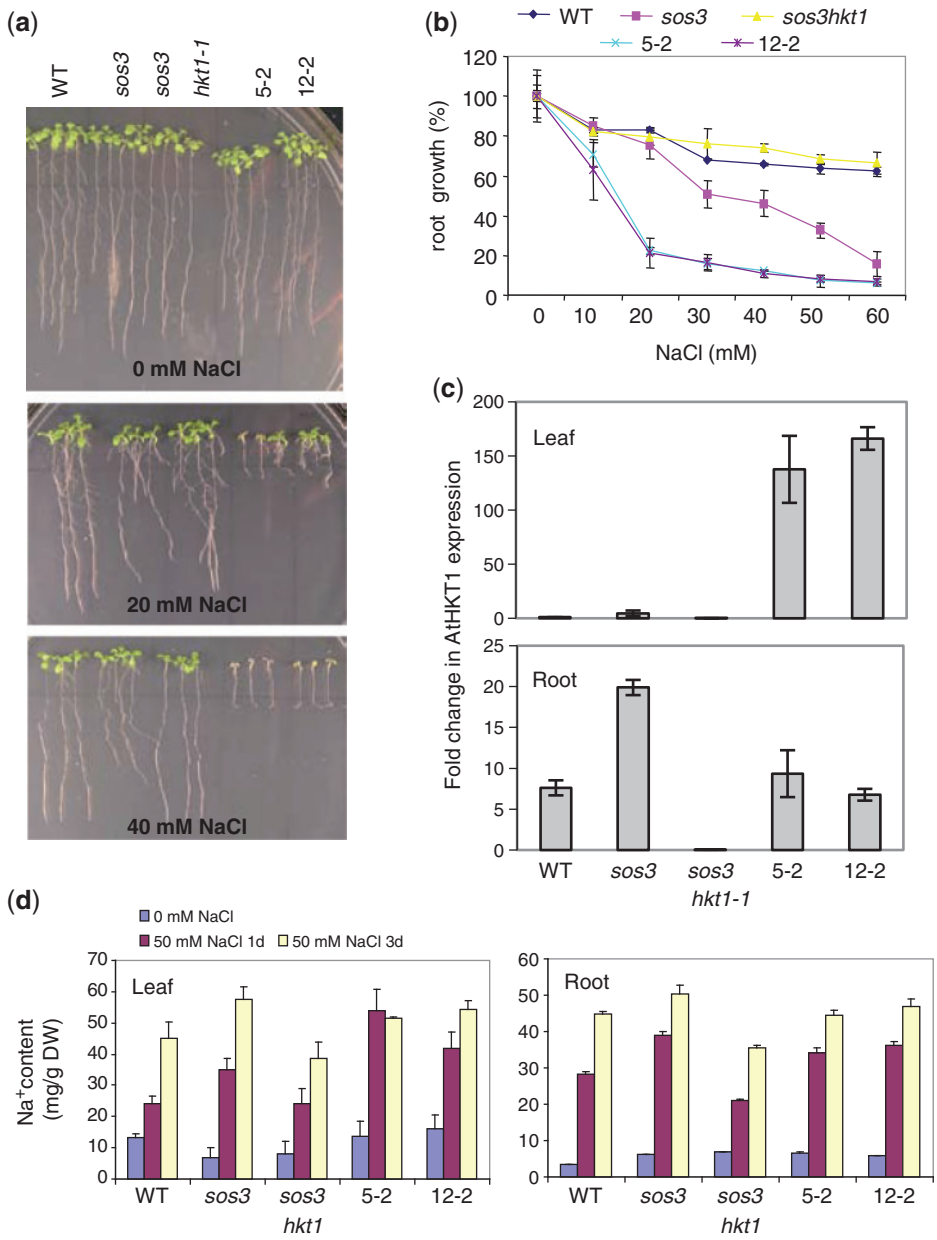

Fig. 4 Effect of *AtHKT1* expression driven by the 2.0 kb promoter lacking the putative small RNA target region and the tandem repeats on salt sensitivity. (a) Lines 5-2 and 12-2 with the 2.0 kb promoter and the entire coding region of *AtHKT1* transformed into *sos3hkt1-1* displayed a hypersensitive phenotype to NaCl. (b) Quantitative measurement of root growth. Relative root growth is the percentage of new root growth at the indicated concentration of NaCl relative to the new root growth without NaCl. Error bars represent the SD ($n = 3$). (c) Transcript levels of *AtHKT1* in the leaf and root of wild-type, *sos3*, *sos3hkt1*, 5-2 and 12-2 determined by quantitative real-time PCR. The expression level was calculated as the level relative to the value of the wild-type leaf. (d) Na^+ contents in leaf and root. Error bars represent the SD ($n = 3$).

the role of the putative small RNA target region and the tandem repeat in *AtHKT1* expression and salt tolerance, a series of deletion constructs with or without the small RNA target sequence and the tandem repeat were generated for genetic complementation tests and GUS fusion analysis. A 3.9 kb *AtHKT1* promoter lacking the tandem repeat with (indicated as 3.9 kb in **Fig. 5**) or without (indicated as 3.9 kb del. sRNA target in **Fig. 5**) the small RNA target region and a 5.2 kb *AtHKT1* promoter containing the tandem repeat with (indicated as 5.2 kb in **Fig. 5**) or without (indicated as 5.2 kb del. sRNA target in **Fig. 5**) the small RNA target region driving the entire *AtHKT1* coding region were transformed into *hkt1-1* and *sos3hkt1-1* mutants and the salt sensitivity of T_2 transgenic seedlings was analyzed by root bending assays. In the *hkt1-1* single mutant background, transgenic seedlings with the 3.9 or 5.2 kb promoter exhibited similar salt sensitivity in root growth

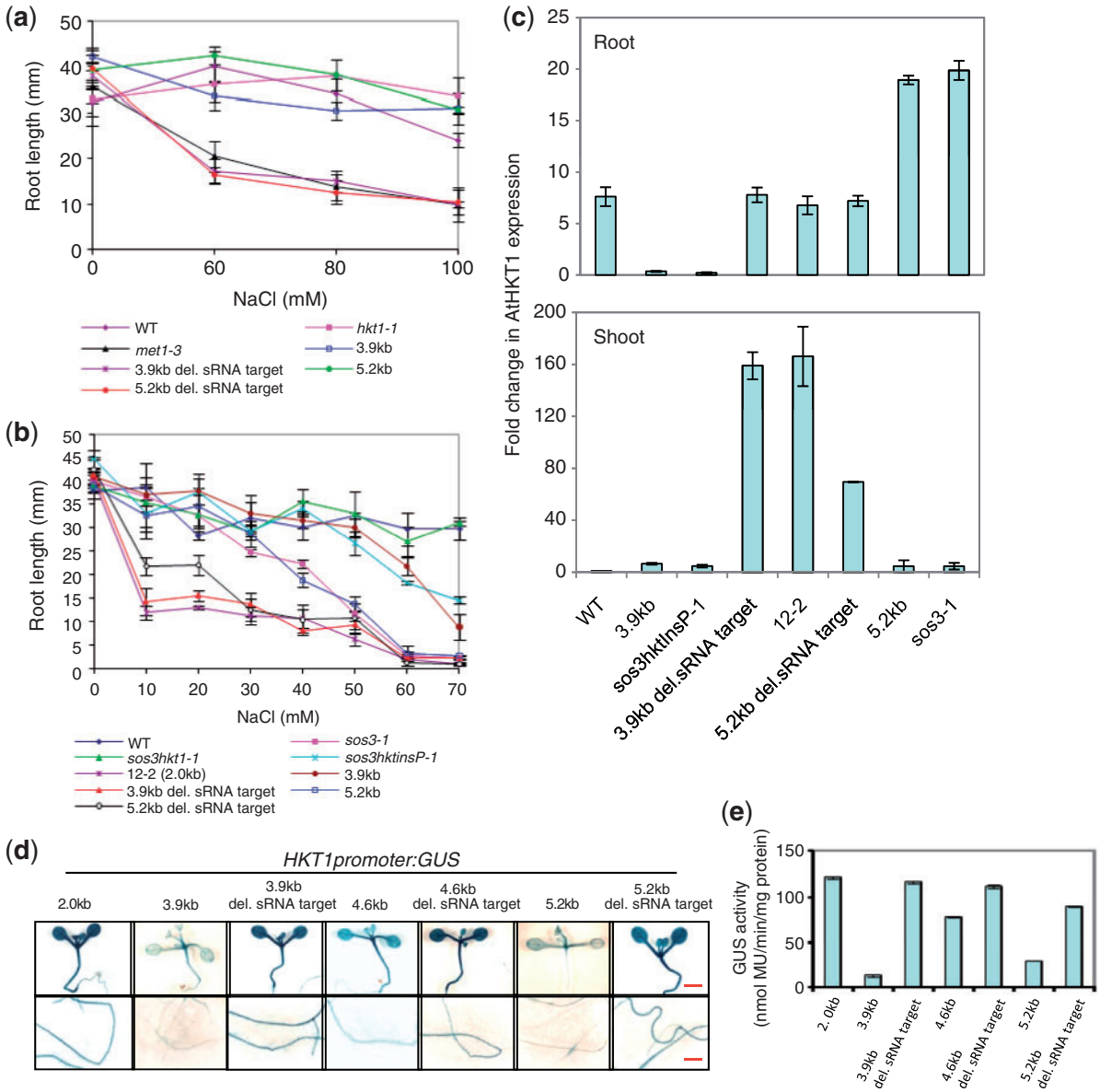

Fig. 5 Role of DNA methylation and the putative small RNA target region in *AtHKT1* gene expression and salt tolerance. (a) Quantitative measurement of root growth showing the salt sensitivity of the wild type, *hkt1-1*, *met1-3* and transgenic lines (in the background of *hkt1-1*) harboring the complementation constructs described in the Materials and Methods. Error bars represent the SD ($n = 5$). (b) Quantitative measurement of root growth showing the salt sensitivity of the wild type, *sos3-1*, *sos3hkt1-1*, *sos3hktInsP-1* and transgenic lines (in the background of *sos3hkt1-1*) harboring the complementation constructs described in the Materials and Methods. Error bars represent the SD ($n = 5$). (c) Transcript levels of *AtHKT1* in the leaf and root of the wild type, *sos3*, and *sos3hkt1-1* harboring the different complementation constructs shown in (b). The expression level was determined by quantitative real-time PCR and was calculated as the level relative to the value of the wild-type leaf. (d) Histochemical staining of GUS of transgenic seedlings harboring different types of *AtHKT1* promoter driving GUS gene expression. At least five transgenic lines were examined and only one line is shown. Top panel, bar = 10 mm; bottom panel, bar = 2.5 mm. (e) GUS activity measurement.

when compared with wild-type and *hkt1-1* seedlings, while transgenic seedlings with the 3.9 or 5.2 kb promoter without the small RNA target region displayed a salt-sensitive phenotype resembling that of the *met1-3* mutant (**Fig. 5a** and Supplementary Fig. S2a). This result suggests that the salt sensitivity of *met1-3* mutant roots is attributed to methylation of the small RNA target region in the *AtHKT1* promoter. In the *sos3hkt1-1* mutant background, the entire *AtHKT1* gene including the 5.2 kb promoter restored the salt sensitivity of *sos3hkt1-1* to levels of the *sos3* mutant, which indicates that the 5.2 kb promoter is a complete promoter controlling the endogenous *AtHKT1* expression. The 3.9 kb promoter plus

the *AtHKT1* coding region only partially complements the *sos3hkt1-1* phenotype, which resembles the phenotype of the weak *sos3* suppressor *sos3hktInsP-1* (**Fig. 5b** and Supplementary Fig. S2b). This result further supports the idea that the tandem repeat present in the 5.2 kb promoter but lacking in the 3.9 kb promoter is required for full expression of the *AtHKT1* gene. Both the 5.2 and 3.9 kb promoter without the putative small RNA target region driving *AtHKT1* expression cannot functionally complement the *sos3hkt1-1* salt-sensitive phenotype and thus it displays even greater salt sensitivity than the *sos3* mutant. The overcomplementation phenotype resembles the transgenic line 12-2 harboring the 2.0 kb promoter plus the coding region (**Fig. 5b** and Supplementary Fig. S2b).

AtHKT1 gene expression analysis (**Fig. 5c**) further supports the complementation results shown in **Fig. 5b**. In roots, the *AtHKT1* transcript level significantly increased in the *sos3* mutant (**Figs. 4c**, **5c**), which indicates that SOS3 plays a role in the transcriptional regulation of *AtHKT1*gene expression. In both roots and leaves, the *AtHKT1*transcript level in complementation transgenic *sos3hkt1-1* plants harboring the 5.2 kb promoter plus the entire coding region (indicated as 5.2 kb) resembles the expression level of the native *AtHKT1* gene in the *sos3* mutant (**Fig. 5c**). This result indicates that the 5.2 kb promoter is indeed a complete promoter for *AtHKT1* expression and regulation. Complementation transgenic plants harboring the 3.9 kb promoter driving *AtHKT1* expression (indicated as 3.9 kb) display an *AtHKT1* expression pattern similar to that in the *sos3hktInsP-1* weak suppressor, while complementation transgenic plants with the 3.9 kb promoter lacking the putative small RNA target region driving *AtHKT1* expression (indicated as 3.9 kb del. sRNA target) resembles 12-2 transgenic complementation plants (**Fig. 5c**). Taken together, these results suggest that the tandem repeat and the putative small RNA target region are important for tissue-specific expression and regulation of *AtHKT1*.

The effect of the tandem repeat and the small RNA target region on gene expression was dissected by promoter–GUS analysis (**Fig. 5d, e**). Compared with the 5.2 kb complete promoter, the 2.0 kb promoter results in a substantial increase in GUS gene expression. The 3.9 kb promoter lacking the tandem repeat has reduced activity to drive GUS expression when compared with the full promoter (**Fig. 5d, e**), which is consistent with the role of the tandem repeat in enhancing gene expression (**Fig. 2d**). Interestingly, the 4.6 kb promoter containing only R2 has increased activity when compared with the 5.2 kb promoter including both R1 and R2 repeat elements (**Fig. 5d, e**), further suggesting that R1 may have a inhibitory role in enhancing function of the tandem repeat. When the putative small RNA target region was deleted from the promoter, the promoter activity driving GUS gene expression was significantly increased, which resembles the 2.0 kb promoter lacking both the tandem repeat and the putative small RNA target (**Fig. 5d, e**).

Discussion

In the present study, we have isolated unique genetic mutants with T-DNA insertions in the promoter of *AtHKT1*, which led to the identification of several important elements in the *AtHKT1* promoter for expression and regulation (**Figs. 1**, **2**). Based on the weak suppression phenotype of *sos3hktInsP-1* and *sos3hktInsP-2*, it is apparent that the distal tandem repeat is required for full expression of *AtHKT1*. The tandem repeat functions as an enhancer element when fused with a minimal 35S promoter (**Fig. 2c, d**). Intriguingly, R1 could not enhance while R2 significantly enhanced reporter gene expression (**Fig. 2c, d**). Although these two repeat elements in the tandem repeat are nearly identical, small differences between these two repeats could still result in differences in DNA modification and binding affinity with *trans*-acting proteins.

Rus et al. (2006) identified *AtHKT1* as the genetic locus driving elevated shoot Na^+ in both Ts-1 and Tsu-1, two coastal populations of Arabidopsis with enhanced Na^+ accumulation. Sequence analysis revealed several major differences between these two wild populations and the Col-0 ecotype in both the promoter and coding region of *AtHKT1*. One of the striking differences is that both Ts-1 and Tsu-1 have only one copy of the tandem repeat. Polymorphisms exist amongst the single copy sequences in Ts-1 and Tsu-1 and R1 and R2 in Col-0, but it appears that the single copy sequence is more similar to R1 from Col-0 (Supplementary Fig. S1). Thus, the single copy sequence in Ts-1 and Tsu-1 might have little enhancing ability for gene expression like R1 does in Col-0. In fact, *AtHKT1* gene expression in roots of Ts-1 and Tsu-1 is clearly lower than that in Col-0 (Rus et al. 2006), which could be attributed to a loss of the enhancing element in the *AtHKT1* promoter in these two coastal ecotypes. Although other major sequence changes in the promoter and coding region of *AtHKT1* in Ts-1 and Tsu-1, including a significant change in the promoter sequence upstream and near the putative TATA box and changes in seven amino acid residues in the AtHKT1 protein, may result in lower expression or less active transport protein, our data, together with the results from Rus et al. (2006), highlight the importance of the tandem repeat in the expression and regulation of *AtHKT1*.

The *AtHKT1* promoter contains a putative small RNA target region where CG methylation in the leaf is higher than that in the root (**Fig. 3a**), which may, at least in part, contribute to higher expression of *AtHKT1* in roots than in leaves (**Fig. 3b**). It has been proven that de novo DNA methylation is guided by siRNAs through RdDM, and the primary players for RdDM are AGO4, RDR2 and DCL3 (Gehring and Henikoff, 2008). In our study, non-CG methylation at CHG and CHH sites is remarkably reduced in the small RNA biogenesis mutant *rdr2*, which indicates that non-CG methylation in this promoter region is directed by small RNAs. The small RNA ASRP-805 complementary to the sequence in this promoter region was detected in Col-0 wild-type plants but was not detectable in the *rdr2* mutant (**Fig. 3c**), further supporting the notion that small RNAs play an important role in *AtHKT1* promoter methylation. Based on

DNA methylation and gene expression data of *AtHKT1* in the wild type, *met1-3*, *rdr2* and complementation lines (**Figs. 3a, b**, and **5**), it is conceivable that DNA methylation, including RdDM, in the putative small RNA target region is important in controlling *AtHKT1* expression and may perform a distinct role in roots and leaves. The expression level of *AtHKT1* in the leaves of *rdr2* is substantially higher than that in wild-type leaves, suggesting that RdDM in the *AtHKT1* promoter plays an inhibitory role in the expression of *AtHKT1* in leaves. On the other hand, loss of both CG and non-CG methylation in the *met1-3* mutant resulted in a increase in *AtHKT1* expression in both roots and leaves (**Fig. 3b**), suggesting that heavy methylation in the promoter region is required to maintain *AtHKT1* expression at a low level and perhaps in a correct pattern in the seedling. Different *AtHKT1* expression patterns in *rdr2* and *met1-3* might be due to differences in methylation of specific sequences in the putative small RNA target region or differences in methylation of other promoter regions, e.g. the tandem repeat.

The importance of DNA methylation in salt tolerance was established by the observation that the *met1-3* mutant is hypersensitive to NaCl (**Fig. 5a** and Supplementary Fig. S2a). Hypersensitivity to NaCl in *met1-3* might be attributed to a loss of methylation in the putative small RNA target region in the *AtHKT1* promoter. This notion is supported by the finding that the *AtHKT1* promoter without the putative small RNA target region driving the entire *AtHKT1* gene expression resulted in a similar salt-sensitive phenotype to *met1-3* (**Fig. 5a** and Supplementary Fig. S2a). Intriguingly, the *rdr2* mutant did not show a salt-sensitive phenotype in the root bending assay although non-CG methylation in the putative small RNA target region is remarkably reduced. Perhaps de novo methylation of the *AtHKT1* promoter rendered by RdDM is to fine-tune the expression of *AtHKT1* in leaves, which may be important merely for long-term adaption of Arabidopsis to salt stress, but not a mechanism for salt tolerance in the short term during a root bending assay. Nevertheless, the putative small RNA target region and presumably its methylation appears to be important to control *AtHKT1* expression in leaves and roots (**Fig 5c–e**). Differential expression of *AtHKT1* in roots and leaves is important for salt tolerance, as suggested by the analysis of lines 5-2 and 12-2. In lines 5-2 and 12-2, the reversed expression pattern of *AtHKT1* in roots and leaves and extremely high transcript level of *AtHKT1* in leaves would lead to the hypersensitive phenotype of these lines to NaCl (**Fig. 4**). The reversed *AtHKT1* expression pattern in these two lines also resulted in the rapid accumulation of Na^+ in the leaves (**Fig. 4d**), which could account for NaCl hypersensitivity for seedling leaves.

Materials and Methods

sos3 suppressor screening and characterization

sos3 suppressors were screened from a T-DNA insertion population in a *sos3* background as described by Rus et al. (2001). Salt sensitivity of *sos3* suppressors was measured by root growth as described by Shi et al. (2002).

Ion content measurements

One-week-old seedlings grown in 1/2 Murahige and Skoog (MS) agar medium (0.7% agar) were transferred to a homemade hydroponic culture container with liquid nutrients (1/10 MS salts). After plants grew for 3 weeks, the liquid nutrient was replaced by 1/10 MS salts plus 50 mM NaCl for salt treatment. Roots and shoots were separately harvested and dried at 80°C for at least 2 d. The xylem sap was collected as described by Shi et al. (2002). Ion content measurement was performed according to Shi et al. (2002).

TAIL-PCR

TAIL-PCR was essentially performed as described by Liu et al. (1995). The three primers corresponding to the border sequence of the vector pSKI15 used for T-DNA insertion mutagenesis of *sos3* mutant are as follows: AtLB1, 5′-ATACGACGGATCGTCATTTGTC-3′; AtLB2, 5′-TAATAACGCTGCGGACATCTAC-3′; and AtLB3, 5′-TTGACCATCATACTCATTGCTG-3′. The degenerate primer used for TAIL-PCR amplification was WGCNAGTNAGWANAAG (W = A/T; N = A/T/G/C).

Complementation test

Genetic complementation among weak and strong *sos3* suppressors was determined by genetic crosses and subsequent root growth assay of the F_1 seedlings on 1/2 MS agar medium with 55 or 75 mM NaCl. For molecular complementation, a DNA fragment containing the 2.0 kb promoter region, the entire open reading frame sequence and 523 bp downstream sequence of the stop condon of the *AtHKT1* gene was cloned into the plant binary vector pCAMBIA 2300 as described by Rus et al. (2004) and was named pCAMBIA2300P2.0kb. The complementation constructs with longer promoter sequences were created based on pCAMBIA2300P2.0kb. The promoter region from 3,871 to 2,015 bp upstream of the start codon was amplified and inserted into pCAMBIA2300P2.0kb, producing the 3,871 bp promoter fused with the entire coding region of *AtHKT1*, which was designated as pCAMBIA2300P3.9kb. The tandem repeat was amplified and inserted into pCAMBIA2300P3.9kb to create a full complementation construct pCAMBIA2300P5.2kb. To eliminate the small RNA target region (61 bp) in the promoter, the fragment with the 2.0 kb promoter and 245 bp downstream of the ATG start codon (utilizing the endogenous *Sal*I site here in the *AtHKT1* coding region) in pCAMBIA2300P2.0kb was removed by digestion with *Pst*I and *Sal*I; the remaining vector was ligated to the fragment (2,607 bp upstream and 245 bp downstream of the start codon) digested with *Pst*I and *Sal*I, creating a vector named as pCAMBIA2300P2.6kb for further use. A fragment (from 3,871 to 2,669 bp upstream of the start codon) was amplified and inserted into the vector pCAMBIA2300P2.6kb to create a construct with the 3.9 kb

promoter lacking the putative small RNA target region named pCAMBIA2300P3.9kb-del-sRNA. The tandem repeat was amplified and inserted into pCAMBIA2300P3.9kb-del-sRNA to create pCAMBIA2300P5.2kb-del-sRNA, which contains the 5.2 kb promoter but lacks the putative small RNA target region. These constructs were introduced into *Agrobacterium tumefaciens* strain GV3101 and transformed into *hkt1-1* and *sos3hkt1-1* mutant plants by the flower dipping method (Zhang et al. 2006).

GUS assay

Approximately 50 bp of minimal 35S promoter sequence including the TATA box was synthesized and inserted into pCAMBIA 1381Z, resulting in a transcriptional fusion of the minimal 35S promoter and GUS reporter gene and named mi35S–GUS. The minimal 35S promoter provides a transcription initiation site for the expression of the GUS reporter gene. R1 and R2 were amplified by PCR and cloned into the mi35S–GUS vector separately or as a tandem repeat in front of mi35S promoter to create R1-Mi–GUS, R2-Mi–GUS and R1R2-Mi–GUS constructs. The construction of the *AtHKT1* promoter–GUS fusions with or without the tandem repeat and the putative small RNA target region is as follows. The promoter region (2,014 bp upstream of the start codon) was amplified and inserted into the vector pCAMBIA1381Z to create a 2.0 kb *AtHKT1* promoter–GUS fusion construct named pCAMBIA1381Z2.0kb. The promoter region (3,871 bp upstream of the start codon) was amplified and inserted into pCAMBIA1381Z to create pCAMBIA1381Z3.9kb. R2 was amplified and inserted into pCAMBIA1381Z3.9kb to form pCAMBIA1381Z4.6kb, and the entire tandem repeat (R1R2) was amplified and inserted into pCAMBIA1381Z3.9 kb to create pCAMBIA1381Z5.2kb. To eliminate the small RNA target region (61 bp) in the promoter, a fragment containing 2,607 bp upstream of the start codon was amplified and inserted into pCAMBIA1381Z and named pCAMBIA1381ZP2.6kb; the second fragment (from 3,871 to 2,669 bp upstream of the start codon) was amplified and inserted into the vector pCAMBIA1381ZP2.6 kb to form pCAMBIA1381Z3.9kb-del-sRNA. The 4.6 and 5.2 kb promoters without the putative small RNA target region were constructed in a similar way to that described above and named pCAMBIA1381Z4.6kb-del-sRNA and pCAMBIA1381Z5.2kb-del-sRNA, respectively. The constructs were introduced into *A. tumefaciens* GV3101 and then transferred into Arabidopsis Col-0 wild-type plants. At least six T_2 individual transgenic lines for each construct were subjected to GUS assay. Histochemical staining of GUS was carried out as described (Shi et al. 2002). Quantitative GUS activity assay was carried out according to Weigel and Glazebrook (2002).

Bisulfite genomic DNA sequencing

Ten-day-old seedlings of wild-type and mutants grown on 1/2 MS agar medium were used for DNA isolation. Genomic DNA was extracted from three replicates and purified from root and leaf separately. A 2 μg aliquot of genomic DNA from a mixture of three replicates was used for bisulfite treatment using an EpiTect Bisulfite kit (Qiagen) following the supplier's instructions. The bisulfite conversion thermal cycling conditions were as follows: 99°C for 5 min, 60°C for 25 min, 99°C for 5 min, 60°C for 85 min, 99°C for 5 min, 60°C for 175 min and 20°C overnight. A 5 μl aliquot of purified bisulfite-treated DNA was used as template for the primer extension reaction by using the reverse primer only. The reverse primer is 5′-TTTTCACTTRC AATTACCTTTTTACCCATT-3′ (R = A/G). After the primer extension reaction (10 cycles of 95°C for 1 min, 60°C for 3 min, 72°C for 3 min), the forward primer (5′-TATGAGAAYT AATAATTTGTTATATGAAAA-3′; Y = C/T) was added into the reaction mixture and the second PCR was as follows: 10 cycles of 95°C for 1 min, 60°C for 1.5 min and 72°C for 2 min, 30 cycles of 95°C for 1 min, 50°C for 1.5 min and 72°C for 2 min, and one cycle of 72°C for 10 min. The PCR product was used as template for an additional amplification by using a pair of nested primers (forward primer, 5′-GTGTAATTTATAAAAGTAGTATGGTAA AAAAG-3′; reverse primer, 5′-ATCACATAAAACACTTAAATA ATTTCATAA-3′). PCR products were purified and cloned into pGEM T-vector (Promega). About 15 independent clones from each PCR product were sequenced.

Quantitative real-time PCR

Ten-day-old seedlings grown in 1/2 MS agar (0.7%) medium were collected for RNA isolation. Total RNA was extracted from roots and leaves using an RNeasy Plant Mini kit (Qiagen). First-strand cDNA was synthesized from 2 μg of total RNA using M-MLV-Reverse Transcriptase and Oligo $(dT)_{15}$ primer (Promega). Quantitative real-time PCR was carried out by using ABI PRISM 7500 Real-Time PCR Systems (Applied Biosystems) and the iTaq™ SYBR Green Supermix with the ROX kit (Bio-Rad) following a standard protocol. The primers for real-time PCR were designed by using the PrimerQuest program (Integrated DNA Technology). The following primers were used: ACTIN2-F, 5′-ACACTGTGCCAATCT ACGAGGGTT-3′; ACTIN2-R, 5′-ACAATTTCCCGCTCTGCTGT TGTG-3′; HKT1-F, 5′-CATCACTCTCGAAGTTATCAGTGCATA TG-3′; and HKT1-R, 5′-TTAGTACGAATTTTCCCATTGGACTC C-3′. The relative expression level of each sample was calculated and analyzed from three independent reactions.

Small RNA blot analysis

RNA was extracted from Arabidopsis seedlings by using Plant RNA Reagent (Invitrogen). Small RNA detection using Northern blot was performed according to Xie et al. (2005). A locked nucleic acid (LNA)-modified detection probe (Exiqok) complementary to the small RNA ASRP-805 (5′-AUC UUCCACCAUCACAACCACCAG-3′) was used as probe for ASRP-805 detection. An oligonucleotide probe specific to miRNA163 (5′-UUGAAGAGGACUUGGAACUUCGAU-3′) was used for miRNA 163 detection.

Supplementary data

Supplementary data are available at PCP online.

Funding

This work was supported by the the US Department of Agriculture [National Research Initiative projects 2004-35100-14863 and 2007-35100-18378 to H.S.]; Rural Development Administration [Biogreen 21 Project (20070301034030) to D.B.]; Korea Science and Engineering Foundation (KOSEF) [Environmental Biotechnology National Core Research Center Project (R15-2003-012-01002-00) to D.B.].

Acknowledgments

We are very grateful to Drs. Ray Bressan and Mike Hasegawa of Purdue University for providing *sos3* suppressors, to Dr. Zhixin Xie at Texas Tech University for technical support on small RNA analysis, to Dr. Hidetoshi Saze for providing *met1-3* seeds, and to Dr. Paul Pare at Texas Tech University for critical reading of this manuscript.

References

Apse, M.P., Aharon, G.S., Snedden, W.A. and Blumwald, E. (1999) Salt tolerance conferred by overexpression of a vacuolar Na^+/H^+ antiport in Arabidopsis. *Science* 285: 1256–1258.

Berthomieu, P., Conejero, G., Nublat, A., Brackenbury, W.J., Lambert, C., Savio, C. et al. (2003) Functional analysis of *AtHKT1* in Arabidopsis shows that Na^+ recirculation by the phloem is crucial for salt tolerance. *EMBO J.* 22: 2004–2014.

Blumwald, E., Aharon, G.S. and Apse, M.P. (2000) Sodium transport in plant cells. *Biochim. Biophys. Acta* 1465: 140–151.

Chung, J.S., Zhu, J.K., Bressan, R.A., Hasegawa, P.M. and Shi, H. (2008) Reactive oxygen species mediate Na^+-induced *SOS1* mRNA stability in Arabidopsis. *Plant J.* 53: 554–565.

Davenport, R.J., Muñoz-Mayor, A., Jha, D., Essah, P.A., Rus, A. and Tester, M. (2007) The Na^+ transporter AtHKT1;1 controls retrieval of Na^+ from the xylem in Arabidopsis. *Plant Cell Environ.* 30: 497–507.

Gaxiola, R.A., Rao, R., Sherman, A., Grisafi, P., Alper, S.L. and Fink, G.R. (1999) The *Arabidopsis thaliana* proton transporters, AtNhx1 and Avp1, can function in cation detoxification in yeast. *Proc. Natl Acad. Sci. USA* 96: 1480–1485.

Gehring, M. and Henikoff, S. (2008) DNA methylation and demethylation in Arabidopsis: May 23, 2008. *In* The Arabidopsis Book. American Society of Plant Biologists, Rockville, MD; doi: 10.1199/tab.0102, http://www.aspb.org/publications/arabidopsis/.

Henderson, I.R. and Jacobsen, S.E. (2007) Epigenetic inheritance in plants. *Nature* 447: 418–424.

Horie, T., Hauser, F. and Schroeder, J.I. (2009) HKT transporter-mediated salinity resistance mechanisms in *Arabidopsis* and monocot crop plants. *Trends Plant Sci.* 14: 660–668.

Laurie, S., Feeny, K.A., Maathuis, F.J.M., Heard, P.J., Brown, S.J. and Leigh, R.A. (2002) A role of HKT1 in sodium uptake by wheat roots. *Plant J.* 32: 139–149.

Liu, Y.G., Mitsukawa, N., Oosumi, T. and Whittier, R.F. (1995) Efficient isolation and mapping of *Arabidopsis thaliana* T-DNA insert junctions by thermal asymmetric interlaced PCR. *Plant J.* 8: 457–463.

Mäser, P., Eckelman, B., Vaidyanathan, R., Horie, T., Firbairn, D.J., Kubo, M. et al. (2002) Altered shoot/root Na^+ distribution and bifurcating salt sensitivity in *Arabidopsis* by genetic disruption of the Na^+ transporter *AtHKT1*. *FEBS Lett.* 531: 157–161.

Møller, I.S., Gilliham, M., Jha, D., Mayo, G.M., Roy, S.J., Coates, J.C. et al. (2009) Shoot Na^+ exclusion and increased salinity tolerance engineered by cell type-specific alteration of Na^+ transport in Arabidopsis. *Plant Cell* 21: 2163–2178.

Munns, R. and Tester, M. (2008) Mechanisms of salinity tolerance. *Annu. Rev. Plant Biol.* 59: 651–681.

Nublat, A., Desplants, J., Casse, F. and Betthomieu, P. (2001) *sas1*, an *Arabidopsis* mutant overaccumulating sodium in the shoot, shows deficiency in the control of the root radial transport of sodium. *Plant Cell* 13: 125–137.

Plett, D.C. and Møller, I.S. (2010) Na^+ tramsport in glycophytic plants: what we know and would like to know. *Plant Cell Environ.* 33: 612–626.

Rus, A., Baxter, I., Muthukumar, B., Gustin, J., Lahner, B., Yakubova, E. et al. (2006) Natural variants of *AtHKT1* enhance Na^+ accumulation in two wild populations of Arabidopsis. *PLoS Genet.* 2: e210.

Rus, A., Lee, B.H., Muñoz-Mayor, A., Sharkhuu, A., Miura, K., Zhu, J.K. et al. (2004) AtHKT1 facilitates Na^+ homeostasis and K^+ nutrition in planta. *Plant Physiol.* 136: 2500–2511.

Rus, A., Yokoi, S., Sharkhuu, A., Reddy, M., Lee, B-H., Matsumoto, T.K. et al. (2001) AtHKT1 is a salt tolerance determinant that controls Na^+ entry into plant roots. *Proc. Natl Acad. Sci. USA* 98: 14150–14155.

Shi, H., Bressan, R., Hasegawa, P.M. and Zhu, J.-K. (2005) Sodium. *In* Plant Nutritional Genomics. Edited by Broadley, M. and White, P. pp. 127–149. Blackwell Publishing, London.

Shi, H., Ishitani, M., Kim, C. and Zhu, J.-K. (2000) The *Arabidopsis thaliana* salt tolerance gene *SOS1* encodes a putative Na^+/H^+ antiporter. *Proc. Natl Acad. Sci. USA* 97: 6896–6901.

Shi, H., Lee, B.H., Wu, S.J. and Zhu, J.K. (2003) Overexpression of a plasma membrane Na^+/H^+ antiporter gene improves salt tolerance in *Arabidopsis thaliana*. *Nat. Biotechnol.* 21: 81–85.

Shi, H., Quintero, F.J., Pardo, J.M. and Zhu, J.-K. (2002) The putative plasma membrane Na^+/H^+ antiporter SOS1 controls long-distance Na^+ transport in plants. *Plant Cell* 14: 465–477.

Sunarpi., Horie, T., Motoda, J., Kubo, M., Yang, H., Yoda, K. et al. (2005) Enhanced salt tolerance mediated by AtHKT1 transporter-induced Na unloading from xylem vessels to xylem parenchyma cells. *Plant J.* 44: 928–938.

Weigel, D. and Glazebrook, J. (2002) Arabidopsis: A Laboratory Manual. Cold Spring Harbor Laboratory Press, Cold Spring Harbor, NY.

Wierzbicki, A.T., Haag, J.R. and Pikaard, C.S. (2008) Noncoding transcription by RNA polymerase Pol IVb/Pol V mediates transcriptional silencing of overlapping and adjacent genes. *Cell* 135: 635–648.

Xie, Z., Allen, E., Wilken, A. and Carrington, J.C. (2005) DICER-LIKE 4 functions in trans-acting small interfering RNA biogenesis and vegetative phase change in *Arabidopsis thaliana*. *Proc. Natl Acad. Sci. USA* 102: 12984–12989.

Xie, Z. and Qi, X. (2008) Diverse small RNA-directed silencing pathways in plants. *Biochim. Biophys. Acta* 1779: 720–724.

Zhang, H.X. and Blumwald, E. (2001) Transgenic salt-tolerant tomato plants accumulate salt in foliage but not in fruit. *Nat. Biotechnol.* 19: 765–768.

Zhang, H.X., Hodson, J.N., Williams, J.P. and Blumwald, E. (2001) Engineering salt-tolerant Brassica plants: characterization of yield and seed oil quality in transgenic plants with increased vacuolar sodium accumulation. *Proc. Natl Acad. Sci. USA* 98: 12832–12836.

Zhang, X., Henriques, R., Lin, S.S., Niu, Q.W. and Chua, N.H. (2006) *Agrobacterium*-mediated transformation of *Arabidopsis thaliana* using the floral dip method. *Nat. Protoc.* 1: 641–646.